Joint Vehicle Tracking and RSU Selection for V2I Communications with Extended Kalman Filter

Jiho Song, *Member, IEEE,* Seong-Hwan Hyun, *Student Member, IEEE,* Jong-Ho Lee, *Member, IEEE,* Jeongsik Choi, *Member, IEEE,* and Seong-Cheol Kim, *Senior Member, IEEE*

***Abstract*—We develop joint vehicle tracking and road side unit (RSU) selection algorithms suitable for vehicle-to-infrastructure (V2I) communications. We first design an analytical framework for evaluating vehicle tracking systems based on the extended Kalman filter. A simple, yet effective, metric that quantifies the vehicle tracking performance is derived in terms of the angular derivative of a dominant spatial frequency. Second, an RSU selection algorithm is proposed to select a proper RSU that enhances the vehicle tracking performance. A joint vehicle tracking algorithm is also developed to maximize the tracking performance by considering sounding samples at multiple RSUs while minimizing the amount of sample exchange. The numerical results verify that the proposed vehicle tracking algorithms give better performance than conventional signal-to-noise ratio-based tracking systems.**

***Index Terms*—Joint vehicle tracking, road side unit selection, extended Kalman filter, millimeter wave V2I communications**

I. Introduction

Vehicle-to-everything (V2X) communications are a promising candidate to facilitate intelligent transport systems required for fully connected vehicular networks [1], [2]. Vehicles can obtain traffic information beyond the sensing range of radar and LIDAR via wireless communication networks [3]. V2X-assisted collaborate sensing are thought to be one of the key enabling technologies in fully automated driving [4]. The enhanced traffic situational awareness via a wireless network would create new services, e.g., vehicular platoon driving [5]. Vehicular communication networks are a prime technology for supporting intelligent transportation system.

Securing a seamless radio connection is a significant challenge in vehicle-to-infrastructure (V2I) communication networks. Such connections are required to utilize a wide bandwidth in the millimeter-wave (mmWave) spectrum because a large amount of sensor data must be exchanged [3]. The vehicular channels at mmWave frequencies may change rapidly because the relative velocity between vehicles and a mounted road side unit (RSU) becomes large compared to conventional mobile systems. Unpredictable vehicle movements make it difficult to estimate future trajectories of fast-moving vehicles [6]. Fast and reliable vehicle tracking is essential to cope with channel fluctuations [7]. The challenge in V2I communications is to maintain wireless connections while satisfying these conflicting requirements for vehicle tracking [8].

Assuming a single cell network, vehicle tracking algorithms, which can be incorporated in current cellular networks, have been developed based on the extended Kalman filter (EKF) [9], [10]. In V2I networks, RSUs must be densely deployed to avoid an intermittent disconnection of the radio link [11]. A handover between RSUs frequently occurs due to the high mobility characteristics of vehicular channels [12]. The road environment with densely deployed RSUs necessitates the development of a fast and reliable RSU selection algorithm to secure a seamless radio connection. Considering a multi-connectivity framework, a joint vehicle tracking algorithm is also needed to maximize the vehicle tracking performance.

Coordinated multi-point transmission algorithms have been studied extensively to enhance network throughput [13]. Conventional multi-transmission systems are designed based on an average signal-to-noise ratio (SNR) metric that is suitable for evaluating cellular networks with a circular shape service area. On the other hand, the shape of the service area in V2I networks is very different from cellular networks because most roads are very narrow and RSUs are installed near the road [10]. Therefore, the SNR-based transmission systems may be unsuitable for V2I networks. Furthermore, the tight budget constraints of RSUs necessitate the redesign of communication systems cost-effectively to enable low latency communications using low-cost transceivers.

In this paper, we aim to develop an analytical framework of joint vehicle tracking and RSU selection for V2I communications. First, we design a simple metric to quantify a vehicle tracking performance accurately by considering the unique shape of a service area in V2I networks. To the best of the author's knowledge, a vehicle tracking performance metric has not yet been designed in terms of the angular variation in a spatial frequency domain. Second, based on the proposed metric, an RSU selection algorithm is developed for providing a seamless handover between neighboring RSUs. Lastly, a joint vehicle tracking algorithm is developed to maximize tracking performance by considering angular variations obtained from multiple RSUs while minimizing the amount of data exchange.

J. Song is with the School of Electrical Engineering, University of Ulsan, Ulsan 44610, South Korea (e-mail: jihosong@ulsan.ac.kr).

S.-H. Hyun and S.-C. Kim are with the School of Electrical Engineering, Seoul National University, and also with the Institute of New Media & Communications (INMC), Seoul 08826, South Korea (e-mail: {shhyun, sckim}@maxwell.snu.ac.kr).

J.-H. Lee is with the School of Electronic Engineering, Soongsil University, Seoul 06978, South Korea (e-mail: jongho.lee@ssu.ac.kr).

J. Choi is with the School of Electronics Engineering, Kyungpook National University, Daegu 41566 (e-mail: jeongsik.choi@knu.ac.kr).

This work was supported by the 2020 Research Fund of University of Ulsan.
(Corresponding author: Jong-Ho Lee.)

This article has been accepted for publication in IEEE Transactions on Vehicular Technology. This is the author's version which has not been fully edited and content may change prior to final publication. Citation information: DOI 10.1109/TVT.2022.3153345

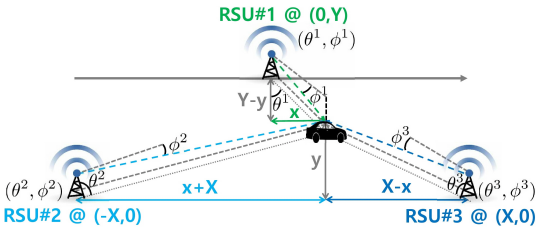

Fig. 1. An overview of V2I communication system.

II. System Model

We consider a vehicle tracking system designed based on the EKF with uplink channel sounding samples. Considering a multiple-input single-output system using M transmit antennas, an input-output expression for the ℓ-th received sounding sample is defined by

$$r_\ell^u = \sqrt{\rho_\ell^u}\mathbf{z}_\ell^u\mathbf{h}_\ell^u + n_\ell^u,$$

where $u \in \{1,\cdots,U\}$ is the index for the RSU, $r_\ell^u = r_\ell^{u,\text{re}} + jr_\ell^{u,\text{im}} \in \mathbb{C}$ is the received sounding sample, $\mathbf{z}_\ell^u = \mathbf{z}_\ell^{u,\text{re}} + j\mathbf{z}_\ell^{u,\text{im}} \in \mathbb{C}^{1\times M}$ is the unit-norm combing vector at the RSU, $\mathbf{h}_\ell^u = \mathbf{h}_\ell^{u,\text{re}} + j\mathbf{h}_\ell^{u,\text{im}} \in \mathbb{C}^M$ is the channel vector, and $n_\ell^u = n_\ell^{u,\text{re}} + jn_\ell^{u,\text{im}} \sim \mathcal{CN}(0,1)$ is the normalized (combined) noise that follows complex Gaussian distribution with zero mean and unit variance. The average SNR is $\rho_\ell^u \doteq \frac{\varrho \text{G}_{\text{tx}}\text{G}_{\text{rx}}}{\sigma_{\text{n}}^2}\left(\frac{\lambda}{4\pi d_\ell^u}\right)^n \overset{(a)}{=} \frac{\varrho}{\sigma_{\text{n}}^2}\left(\frac{\lambda}{4\pi d_\ell^u}\right)^n$, where ϱ is the transmit power, σ_{n}^2 is the noise power, d_ℓ^u is the distance between a vehicle and the u-th RSU, λ is the wavelength of the radio signals, and n is the path-loss exponent. Note that $\text{G}_{\text{tx}} = \text{G}_{\text{rx}} = 1$ is assumed in (a) to simplify the presentation. By decomposing all the variables into real and imaginary parts, the input-output expression is rewritten in the real domain, as

$$\tilde{\mathbf{r}}_\ell^u = \sqrt{\rho_\ell^u}\tilde{\mathbf{Z}}_\ell^u\tilde{\mathbf{h}}_\ell^u + \tilde{\mathbf{n}}_\ell^u, \tag{1}$$

where $\tilde{\mathbf{r}}_\ell^u = [r_\ell^{u,\text{re}}, r_\ell^{u,\text{im}}]^T \in \mathbb{R}^2$, $\tilde{\mathbf{Z}}_\ell^u = \begin{bmatrix} \mathbf{z}_\ell^{u,\text{re}} & -\mathbf{z}_\ell^{u,\text{im}} \\ \mathbf{z}_\ell^{u,\text{im}} & \mathbf{z}_\ell^{u,\text{re}} \end{bmatrix} \in \mathbb{R}^{2\times 2M}$, $\tilde{\mathbf{h}}_\ell^u = [(\mathbf{h}_\ell^{u,\text{re}})^T, (\mathbf{h}_\ell^{u,\text{im}})^T]^T \in \mathbb{R}^{2M}$, and $\tilde{\mathbf{n}}_\ell^u = [n_\ell^{u,\text{re}}, n_\ell^{u,\text{im}}]^T \in \mathbb{R}^2$.

By assuming a line-of-sight channel with a dominant radio path, the channel vector can be modeled by

$$\mathbf{h}_\ell^u \simeq \mathbf{h}(\psi_\ell^u) \doteq \beta_\ell^u \mathbf{d}_M(\psi_\ell^u),$$

where β_ℓ^u is the small-scale channel fading parameter, and $\mathbf{d}_M(\psi_\ell^u) = [1, e^{j\psi_\ell^u}, \cdots, e^{j(M-1)\psi_\ell^u}]^T \in \mathbb{C}^M$ is an array response vector with a spatial frequency, $\psi_\ell^u \in [-\pi, \pi)$. The real and imaginary parts of the array response vector are expressed as

$$\tilde{\mathbf{d}}_M^{\text{re}}(\psi_\ell^u) = \left[\cos(0), \cos(\psi_\ell^u), \cdots, \cos((M-1)\psi_\ell^u)\right]^T \in \mathbb{R}^M,$$
$$\tilde{\mathbf{d}}_M^{\text{im}}(\psi_\ell^u) = \left[\sin(0), \sin(\psi_\ell^u), \cdots, \sin((M-1)\psi_\ell^u)\right]^T \in \mathbb{R}^M.$$

The channel vector is then reformulated in a real domain as

$$\tilde{\mathbf{h}}_\ell^u \simeq \tilde{\mathbf{h}}(\psi_\ell^u) = \begin{bmatrix} \beta_\ell^{u,\text{re}}\tilde{\mathbf{d}}_M^{\text{re}}(\psi_\ell^u) - \beta_\ell^{u,\text{im}}\tilde{\mathbf{d}}_M^{\text{im}}(\psi_\ell^u) \\ \beta_\ell^{u,\text{im}}\tilde{\mathbf{d}}_M^{\text{re}}(\psi_\ell^u) + \beta_\ell^{u,\text{re}}\tilde{\mathbf{d}}_M^{\text{im}}(\psi_\ell^u) \end{bmatrix} \in \mathbb{R}^{2M}.$$

Fig. 1 presents the RSU deployment scenario, where h is the relative height difference between the RSU and vehicles. The position on the y-axis is static because it is assumed that the vehicle does not change the traffic lane. The spatial frequencies for the RSUs can be written by

$$\psi_\ell^1 = \pi \sin\theta_\ell^1 \cos\phi_\ell^1 = \frac{\pi x_\ell}{(x_\ell^2 + (\text{Y}-y)^2 + h^2)^{\frac{1}{2}}} \doteq \text{g}^1(\mathbf{t}_\ell),$$
$$\psi_\ell^2 = \pi \sin\theta_\ell^2 \cos\phi_\ell^2 = \frac{\pi(\text{X}+x_\ell)}{((\text{X}+x_\ell)^2 + y^2 + h^2)^{\frac{1}{2}}} \doteq \text{g}^2(\mathbf{t}_\ell),$$
$$\psi_\ell^3 = \pi \sin\theta_\ell^3 \cos\phi_\ell^3 = \frac{\pi(\text{X}-x_\ell)}{((\text{X}-x_\ell)^2 + y^2 + h^2)^{\frac{1}{2}}} \doteq \text{g}^3(\mathbf{t}_\ell),$$

because the horizontal and vertical angle of departure (AoD) for the u-th RSU, i.e., θ_ℓ^u and ϕ_ℓ^u, are defined as functions of the position variables, (x_ℓ, y), and network parameters, (X, Y, h).

The vehicle movement can be modeled by using the linear state transition model with a sampling period T_s, such as

$$\mathbf{t}_\ell = \mathbf{A}\mathbf{t}_{\ell-1} + \mathbf{b}\alpha + \mathbf{c}_{\ell-1}, \tag{2}$$

where $\mathbf{t}_\ell = [x_\ell, v_\ell]^T \in \mathbb{R}^2$ is the state vector of a vehicle, in which x_ℓ and v_ℓ denote a position on the x-axis and the velocity of the vehicle at the ℓ-th channel use, and $\alpha \sim \mathcal{N}(0, \sigma_\alpha^2)$ is the acceleration parameter that follows Gaussian distribution with zero mean and variance σ_α^2 [10]. A state transition matrix, an acceleration transition vector, and an error transition vector are defined as, $\mathbf{A} = \begin{bmatrix} 1 & T_s \\ 0 & 1 \end{bmatrix} \in \mathbb{R}^{2\times 2}$, $\mathbf{b} = \left[\frac{T_s^2}{2}, T_s\right]^T \in \mathbb{R}^2$, and $\mathbf{c}_{\ell-1} \sim \mathcal{N}(\mathbf{0}_2, \mathbf{Q}_\omega)$, respectively [14]. Similar to [9], the covariance matrices for the acceleration transition vector and the error transition vector are modeled by $\mathbf{Q}_\alpha = \mathbf{b}\mathbf{b}^T\sigma_\alpha^2 \in \mathbb{R}^{2\times 2}$ and $\mathbf{Q}_\omega = \sigma_\omega^2 \text{diag}[T_s^2, 1] \in \mathbb{R}^{2\times 2}$, respectively. It is assumed that $\mathbf{c}_{\ell-1}$ is dynamic, while α is static in each coherence time.

This paper reviews a vehicle tracking algorithm developed based on the EKF [10]. Assuming the u-th RSU is used for vehicle tracking, the initial state information of a vehicle, (x_0, y, v_0), is fed back to the RSU. Furthermore, it is assumed that channel fading information, $(\rho_\ell^u, \beta_\ell^u)$, is known at the RSU.

1) State prediction process: Since RSU does not have information on the acceleration and error transition vectors, the vehicle state vector is predicted based on the state transition model as follows:

$$\hat{\mathbf{t}}_{\ell|\ell-1}^u = \mathbf{A}\hat{\mathbf{t}}_{\ell-1}^u, \tag{3}$$

where $\hat{\mathbf{t}}_{\ell-1}^u$ is the state vector estimated at discrete time $\ell-1$. Without correcting the transition errors, the covariance matrix of the prediction error will be updated as $\hat{\mathbf{Q}}_{\ell|\ell-1}^u = \mathbf{A}\hat{\mathbf{Q}}_{\ell-1}^u\mathbf{A}^T + \mathbf{Q}_\text{e}$, where $\hat{\mathbf{Q}}_{\ell-1}^u$ is the estimated covariance matrix at a discrete time $\ell-1$, and $\mathbf{Q}_\text{e} = \mathbf{Q}_\alpha + \mathbf{Q}_\omega$.

2) State update process: The predicted state vector will be refined using the channel sounding sample in (1), such as

$$\hat{\mathbf{t}}_\ell^u = \hat{\mathbf{t}}_{\ell|\ell-1}^u + \tilde{\mathbf{K}}_\ell^u\left(\tilde{\mathbf{r}}_\ell^u - \sqrt{\rho_\ell^u}\tilde{\mathbf{Z}}_\ell^u\tilde{\mathbf{h}}(\hat{\psi}_{\ell|\ell-1}^u)\right), \tag{4}$$

where $\tilde{\mathbf{h}}(\hat{\psi}_{\ell|\ell-1}^u)$ is the ray-like channel that is predicted by using the estimated spatial frequency, $\hat{\psi}_{\ell|\ell-1}^u = \text{g}^u(\hat{\mathbf{t}}_{\ell|\ell-1}^u)$. The combiner at RSU is designed to minimize the trace of the estimated covariance matrix, such that $\tilde{\mathbf{Z}}_\ell^u = \arg\min \text{Tr}\{\hat{\mathbf{Q}}_\ell^u\}$. Please refer to the combiner design process in [10] for $\tilde{\mathbf{Z}}_\ell^u$. The state estimation error is refined as

$$\hat{\mathbf{Q}}_\ell^u = \left(\mathbf{I}_2 - \sqrt{\rho_\ell^u}\tilde{\mathbf{K}}_\ell^u\tilde{\mathbf{Z}}_\ell^u\tilde{\mathbf{D}}_{\ell|\ell-1}^u\right)\hat{\mathbf{Q}}_{\ell|\ell-1}^u,$$

This article has been accepted for publication in IEEE Transactions on Vehicular Technology. This is the author's version which has not been fully edited and content may change prior to final publication. Citation information: DOI 10.1109/TVT.2022.3153345

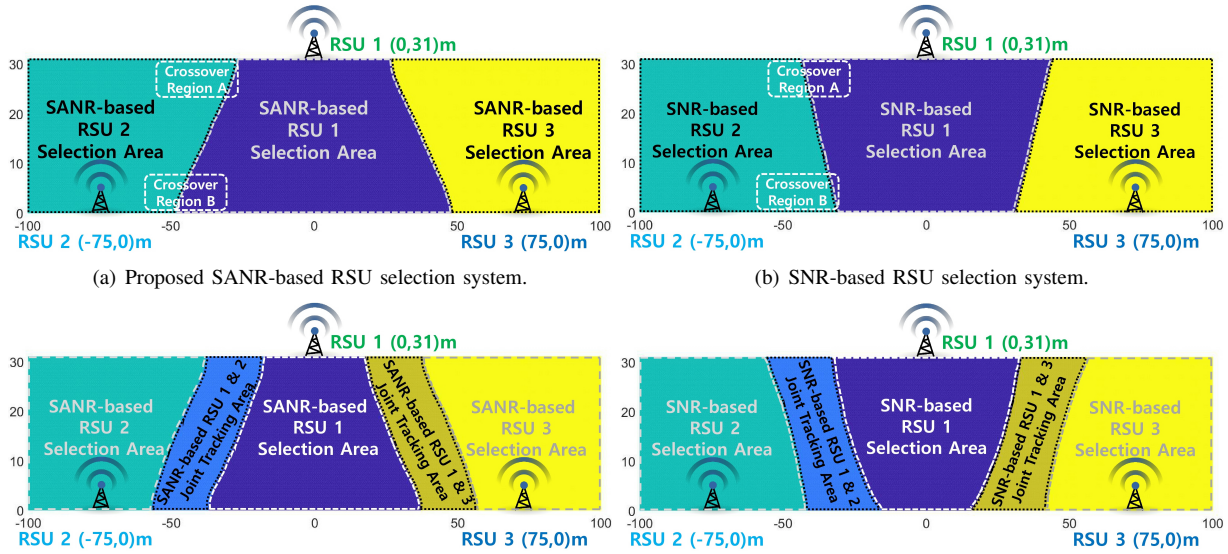

(a) Proposed SANR-based RSU selection system.

(b) SNR-based RSU selection system.

(c) Proposed SANR-based joint tracking system with $\tau_{\text{th}} = 0.98$.

(d) SNR-based joint tracking system with $\tau_{\text{th}} = 0.662$.

Fig. 2. Service areas for EKF-based vehicle tracking systems.

where the Kalman gain matrix is

$$\tilde{\mathbf{K}}^u_\ell = \sqrt{\rho^u_\ell}\hat{\mathbf{Q}}^u_{\ell|\ell-1}(\tilde{\mathbf{Z}}^u_\ell\tilde{\mathbf{D}}^u_{\ell|\ell-1})^T \left(\rho^u_\ell\tilde{\mathbf{Z}}^u_\ell\tilde{\mathbf{D}}^u_{\ell|\ell-1}\hat{\mathbf{Q}}^u_{\ell|\ell-1}(\tilde{\mathbf{Z}}^u_\ell\tilde{\mathbf{D}}^u_{\ell|\ell-1})^T + \mathbf{I}_2/2\right)^{-1}. \quad (5)$$

The Jacobian matrix of the channel is defined by $\tilde{\mathbf{D}}^u_{\ell|\ell-1} = \dot{\mathbf{h}}^u_{\ell|\ell-1}(\dot{\mathbf{g}}^u_{\ell|\ell-1})^T$, where $\dot{\mathbf{h}}^u_{\ell|\ell-1} = \frac{\partial\tilde{\mathbf{h}}(\psi)}{\partial\psi}\Big|_{\psi=\mathrm{g}^u(\hat{\mathbf{t}}^u_{\ell|\ell-1})}$ is the partial derivative of the channel, and the partial derivative of the spatial frequency for the RSUs can be computed as

$$\dot{\mathbf{g}}^u_{\ell|\ell-1} = \frac{\partial \mathrm{g}^u(\mathbf{t})}{\partial \mathbf{t}}\Big|_{\mathbf{t}=\hat{\mathbf{t}}^u_{\ell|\ell-1}} = \pi\dot{\mathrm{g}}^u_{\ell|\ell-1}[1, T_s]^T, \quad (6)$$

$$\dot{\mathrm{g}}^1_{\ell|\ell-1} = ((\mathrm{Y}-y)^2+h^2)(\hat{x}^2_{\ell|\ell-1}+(\mathrm{Y}-y)^2+h^2)^{-\frac{3}{2}},$$
$$\dot{\mathrm{g}}^2_{\ell|\ell-1} = (y^2+h^2)((\mathrm{X}+\hat{x}_{\ell|\ell-1})^2+y^2+h^2)^{-\frac{3}{2}},$$
$$\dot{\mathrm{g}}^3_{\ell|\ell-1} = -(y^2+h^2)((\mathrm{X}-\hat{x}_{\ell|\ell-1})^2+y^2+h^2)^{-\frac{3}{2}}.$$

Please refer to [10] to calculate the Jacobian matrix.

III. RSU Selection Algorithm for V2I Handover

An RSU selection algorithm aims to choose an RSU that can provide the best vehicle tracking performance. In cellular networks, mobile users switch the base station based on the average SNR. Similar to cellular networks, one possible method of RSU selection is to select an RSU that can provide the largest SNR, $u = \max_{u\in\{1,\cdots,U\}}\rho^u_\ell$. With the largest SNR, the service region for RSUs can be defined, as shown in Fig. 2(b).

This paper takes a closer look at the state update process to evaluate the EKF-based vehicle tracking systems analytically. The state update process is designed to correct the state transition error, $\mathbf{e}^u_{\ell|\ell-1} \doteq \mathbf{t}_\ell - \hat{\mathbf{t}}^u_{\ell|\ell-1}$, using channel-sounding samples. In the EKF-based vehicle tracking algorithm, the dominant spatial frequency obtained from a sounding sample will be used to correct the state transition error. The state update process becomes immune to noise as the angular variations caused by vehicle movements become larger. Angular variation might be significantly different depending on the relative location between a vehicle and RSUs, even though the vehicle travels the equivalent distances.

In the state update process, additive noise should be compared with the angular variation instead of evaluating the signal strength of the sounding sample using an average SNR. A new metric is derived to quantify a vehicle tracking performance in terms of an angular variation. In (4), the sounding sample for the u-th RSU is compared with the predicted sample, such as

$$\begin{aligned}\Gamma^u_\ell &= \tilde{\mathbf{r}}^u_\ell - \sqrt{\rho^u_\ell}\tilde{\mathbf{Z}}^u_\ell\tilde{\mathbf{h}}(\hat{\psi}^u_{\ell|\ell-1}) \\ &= \sqrt{\rho^u_\ell}\tilde{\mathbf{Z}}^u_\ell(\tilde{\mathbf{h}}^u_\ell - \tilde{\mathbf{h}}(\hat{\psi}^u_{\ell|\ell-1})) + \tilde{\mathbf{n}}^u_\ell \\ &\overset{(a)}{\simeq} \sqrt{\rho^u_\ell}\underbrace{\tilde{\mathbf{Z}}^u_\ell\tilde{\mathbf{D}}^u_{\ell|\ell-1}\mathbf{e}^u_{\ell|\ell-1}}_{(b)} + \tilde{\mathbf{n}}^u_\ell, \end{aligned} \quad (7)$$

where (a) is derived using the approximated channel vector $\tilde{\mathbf{h}}^u_\ell \simeq \tilde{\mathbf{h}}(\hat{\psi}^u_{\ell|\ell-1}) + \tilde{\mathbf{D}}^u_{\ell|\ell-1}\mathbf{e}^u_{\ell|\ell-1}$, and the predicted channel, $\tilde{\mathbf{h}}(\hat{\psi}^u_{\ell|\ell-1})$, is defined by using the estimated spatial frequency, $\hat{\psi}^u_{\ell|\ell-1} = \mathrm{g}^u(\hat{\mathbf{t}}^u_{\ell|\ell-1})$. The vehicle estimation performance depends on the power ratio between the state-error-correction component[1] in (b) and the noise component. In the following proposition, signal-plus-angular-derivative-to-noise ratio (SANR) is defined as a function of the position variables.

Proposition 1: The SANRs of sounding samples, $\gamma^u_{\ell|\ell-1}$ with $u \in \{1,2,3\}$, are approximated by

$$\gamma^1_{\ell|\ell-1} \simeq \kappa\left((\mathrm{Y}-y)^2+h^2\right)^2\left(\hat{x}^2_{\ell|\ell-1}+(\mathrm{Y}-y)^2+h^2\right)^{-(3+\frac{n}{2})},$$
$$\gamma^2_{\ell|\ell-1} \simeq \kappa\left(y^2+h^2\right)^2\left((\mathrm{X}+\hat{x}_{\ell|\ell-1})^2+y^2+h^2\right)^{-(3+\frac{n}{2})},$$
$$\gamma^3_{\ell|\ell-1} \simeq \kappa\left(y^2+h^2\right)^2\left((\mathrm{X}-\hat{x}_{\ell|\ell-1})^2+y^2+h^2\right)^{-(3+\frac{n}{2})},$$

where $\kappa = \frac{\varrho(M-1)(2M-1)\pi^2\lambda^n(\hat{\mathbf{Q}}_{\ell|\ell-1})_{1,1}}{6(4\pi)^n\sigma^2_{\text{n}}}$.

[1]The state-error-correction component denotes the correlation between the state transition error and the combined Jacobian matrix that includes the derivative of a spatial frequency with respect to a change in the state vector.

This article has been accepted for publication in IEEE Transactions on Vehicular Technology. This is the author's version which has not been fully edited and content may change prior to final publication. Citation information: DOI 10.1109/TVT.2022.3153345

Proof: The SANR of a sounding sample is derived as,

$$\gamma^u_{\ell|\ell-1} = \rho^u_\ell \mathrm{E}\big[\|\tilde{\mathbf{Z}}^u_\ell \tilde{\mathbf{D}}^u_{\ell|\ell-1}\mathbf{e}^u_{\ell|\ell-1}\|_2^2\big] \tag{8}$$
$$\overset{(a)}{=} \frac{\rho^u_\ell}{M}\mathrm{E}\big[(\mathbf{e}^u_{\ell|\ell-1})^T \dot{\mathbf{g}}^u_{\ell|\ell-1}(\dot{\mathbf{h}}^u_{\ell|\ell-1})^T \dot{\mathbf{h}}^u_{\ell|\ell-1}(\dot{\mathbf{g}}^u_{\ell|\ell-1})^T \mathbf{e}^u_{\ell|\ell-1}\big]$$
$$\overset{(b)}{=} \frac{\rho^u_\ell (M-1)(2M-1)\mathrm{E}[(\mathbf{e}^u_{\ell|\ell-1})^T \dot{\mathbf{g}}^u_{\ell|\ell-1}(\dot{\mathbf{g}}^u_{\ell|\ell-1})^T \mathbf{e}^u_{\ell|\ell-1}]}{6},$$

where (a) is because $(\tilde{\mathbf{Z}}^u_\ell)^T\tilde{\mathbf{Z}}^u_\ell = \frac{\mathbf{I}_{2M}}{M}$, and (b) is derived with

$$\mathrm{E}\big[(\dot{\mathbf{h}}^u_{\ell|\ell-1})^T\dot{\mathbf{h}}^u_{\ell|\ell-1}\big] = \mathrm{E}\big[|\beta^{u,\mathrm{re}}_\ell|^2 + |\beta^{u,\mathrm{im}}_\ell|^2\big]\|\dot{\mathbf{d}}_M(\hat{\psi}^u_{\ell|\ell-1})\|_2^2$$
$$= \sum_{m=0}^{M-1} m^2(\sin^2(m\hat{\psi}^u_{\ell|\ell-1}) + \cos^2(m\hat{\psi}^u_{\ell|\ell-1}))$$
$$= \frac{M(M-1)(2M-1)}{6}.$$

The SANR in (8) is approximated by considering $T_s \ll 1$, as

$$\gamma^u_{\ell|\ell-1} \overset{(a)}{\simeq} \frac{\rho^u_\ell (M-1)(2M-1)\pi^2(\dot{\mathrm{g}}^u_{\ell|\ell-1})^2\mathrm{E}[|(\mathbf{e}^u_{\ell|\ell-1})_{1,1}|^2]}{6}$$
$$\overset{(b)}{=} \frac{\varrho(M-1)(2M-1)\pi^2\lambda^n(\dot{\mathrm{g}}^u_{\ell|\ell-1})^2(\hat{\mathbf{Q}}^u_{\ell|\ell-1})_{1,1}}{6(4\pi d^u_\ell)^n\sigma^2_{\mathrm{n}}},$$

where the partial derivative of the spatial frequency, $\dot{\mathbf{g}}^u_{\ell|\ell-1}$, is derived in (6), the approximation in (a) is derived from

$$\dot{\mathbf{g}}^u_{\ell|\ell-1}(\dot{\mathbf{g}}^u_{\ell|\ell-1})^T \simeq \begin{bmatrix} (\pi\dot{\mathrm{g}}^u_{\ell|\ell-1})^2 & 0 \\ 0 & 0 \end{bmatrix},$$

(b) is based on $\rho^u_\ell = \frac{\varrho}{\sigma^2_{\mathrm{n}}}\big(\frac{\lambda}{4\pi d^u_\ell}\big)^n$, and $\mathrm{E}[|(\mathbf{e}^u_{\ell|\ell-1})_{1,1}|^2] = (\hat{\mathbf{Q}}^u_{\ell|\ell-1})_{1,1}$. Note that $(\mathbf{A})_{a,b}$ is the (a,b)-th entry of $\mathbf{A}$. It is assumed that the first element of the covariance matrix are the same, $(\hat{\mathbf{Q}}_{\ell|\ell-1})_{1,1} = (\hat{\mathbf{Q}}^u_{\ell|\ell-1})_{1,1}$ for all $u \in \{1,\cdots,U\}$. ■

Assuming a covariance matrix has arbitrary, but fixed values, the service region is predefined based on SANRs that can be computed using vehicle position variables. For a given predicted state vector, an RSU generating the largest SANR can be chosen based on the predefined service region in Fig. 2(a). For example, vehicles around *Crossover Region A* in Fig. 2 will be connected to RSU 2 based on the predefined service area, even though the vehicles are close to RSU 1. When handover between the RSUs is required, a serving RSU will inform the next RSU of the need for a handover process.

IV. Joint Vehicle Tracking Algorithm

The RSUs near a vehicle can obtain a sounding sample because an omnidirectional antenna, mounted on the roof of vehicles, radiates sounding signals in all directions. It is necessary to develop a joint tracking system to improve the vehicle tracking performance by jointly considering sounding samples at multiple RSUs. One possible approach is to exploit three samples, i.e., $\{\tilde{\mathbf{r}}^1_\ell, \tilde{\mathbf{r}}^2_\ell, \tilde{\mathbf{r}}^3_\ell\}$, obtained from neighboring RSUs. However, this full cooperative tracking solution would impose a burden on the backhaul network because three samples must be shared between RSUs for every sampling period.

This study focuses on developing joint vehicle tracking system to enhance tracking performance while minimizing the amount of sample exchange between neighboring RSUs. A closer look at the full cooperative joint tracking system is needed to define the reference of vehicle tracking performance. Section III introduces the SANR metric to quantify the vehicle tracking performance in terms of the derivative of spatial frequency, which depends on the position variables. Assuming the Kalman gain matrix combines multiple sounding samples optimally, the overall SANR can be defined by $\bar{\gamma} \doteq \sum_{u=1}^3 \gamma^u_{\ell|\ell-1}$. We call the overall SANR of the full cooperative tracking system as the reference SANR.

The overall SANR value depends on the quality of sounding samples used for joint vehicle tracking. We aim to select RSUs as minimal as possible to produce the overall SANR that is greater than the predefined performance threshold τ_{th}, by allowing a small amount of sample-exchange. The SANRs are sorted in descending order, such as $\gamma^{u_1}_{\ell|\ell-1} \geq \gamma^{u_2}_{\ell|\ell-1} \geq \gamma^{u_3}_{\ell|\ell-1}$. If a certain RSU satisfies the predefined performance threshold $\frac{\gamma^{u_1}_{\ell|\ell-1}}{\bar{\gamma}} \geq \tau_{\mathrm{th}}$, only single RSU will be selected for vehicle tracking as $\mathcal{U} = \{u_1\}$. On the other hand, if two RSUs are needed to satisfy the performance threshold $\frac{\gamma^{u_1}_{\ell|\ell-1}}{\bar{\gamma}} < \tau_{\mathrm{th}}$ and $\frac{\gamma^{u_1}_{\ell|\ell-1}+\gamma^{u_2}_{\ell|\ell-1}}{\bar{\gamma}} \geq \tau_{\mathrm{th}}$, a set of selected RSUs will be given by $\mathcal{U} = \{u_1, u_2\}$. If strict subsets of RSUs cannot satisfy the performance threshold, all the RSUs must participate for joint vehicle tracking, such that[2] $\mathcal{U} = \{1,2,3\}$. The service areas for the proposed joint tracking system are predefined based on SANR. Active RSUs for joint tracking will be chosen based

Algorithm 1 Proposed SANR-based joint vehicle tracking

Initialization
1: Initial state vector, $\hat{\mathbf{t}}_0 = [x_0, v_0]^T$
2: Initial covariance matrix, $\hat{\mathbf{Q}}_0 = \mathbf{0}_{2\times 2}$
Linear state prediction
3: Predict state vector, $\hat{\mathbf{t}}_{\ell|\ell-1} = \mathbf{A}\hat{\mathbf{t}}_{\ell-1}$
4: Predict covariance matrix, $\hat{\mathbf{Q}}_{\ell|\ell-1} = \mathbf{A}\hat{\mathbf{Q}}_{\ell-1}\mathbf{A}^T + \mathbf{Q}_{\mathrm{e}}$
RSU selection for joint vehicle tracking
5: Select a set of RSUs, $\mathcal{U}$, based on SANR $\gamma^{u_1} \geq \gamma^{u_2} \geq \gamma^{u_3}$ with $\bar{\gamma} \doteq \sum_u \gamma^u$
6: if $\frac{\gamma^{u_1}}{\bar{\gamma}} \geq \tau_{\mathrm{th}}$, then $\mathcal{U} = \{u_1\}$
7: elseif $\frac{\gamma^{u_1}}{\bar{\gamma}} < \tau_{\mathrm{th}}$ and $\frac{\gamma^{u_1}+\gamma^{u_2}}{\bar{\gamma}} \geq \tau_{\mathrm{th}}$, then $\mathcal{U} = \{u_1, u_2\}$
8: else $\mathcal{U} = \{1,2,3\}$
Uplink channel sounding
9: Selected RSUs compute combiner for sounding, $\tilde{\mathbf{Z}}^u_\ell$
10: Conduct channel sounding, $\tilde{\mathbf{r}}^u_\ell = \sqrt{\rho^u_\ell}\tilde{\mathbf{Z}}^u_\ell\tilde{\mathbf{h}}^u_\ell + \tilde{\mathbf{n}}^u_\ell$
11: Exchange samples, $\tilde{\mathbf{r}}^u_\ell$, between selected RSUs, $u \in \mathcal{U}$
12: Construct overall sample vector, $\tilde{\mathbf{r}}_\ell \in \mathbb{R}^{2|\mathcal{U}|}$
State update based on joint channel sounding
13: Compute overall combiner, $\tilde{\mathbf{Z}}_\ell = \tilde{\mathbf{Z}}^{u_1}_\ell \oplus \cdots \oplus \tilde{\mathbf{Z}}^{u_{|\mathcal{U}|}}_\ell$
14: Design Kalman gain matrix,
$\tilde{\mathbf{K}}_\ell = \hat{\mathbf{Q}}_{\ell|\ell-1}\big((\mathbf{P}^{\frac{1}{2}}_\ell \otimes \mathbf{I}_2)\tilde{\mathbf{Z}}_\ell\tilde{\mathbf{D}}_{\ell|\ell-1}\big)^T\big((\mathbf{P}^{\frac{1}{2}}_\ell \otimes \mathbf{I}_2)\tilde{\mathbf{Z}}_\ell$
$\tilde{\mathbf{D}}_{\ell|\ell-1}\hat{\mathbf{Q}}_{\ell|\ell-1}\big((\mathbf{P}^{\frac{1}{2}}_\ell \otimes \mathbf{I}_2)\tilde{\mathbf{Z}}_\ell\tilde{\mathbf{D}}_{\ell|\ell-1}\big)^T + \mathbf{I}_{2|\mathcal{U}|}/2\big)^{-1}$
15: Update state vector,
$\hat{\mathbf{t}}_\ell = \hat{\mathbf{t}}_{\ell|\ell-1} + \tilde{\mathbf{K}}_\ell(\tilde{\mathbf{r}}_\ell - (\mathbf{P}^{\frac{1}{2}}_\ell \otimes \mathbf{I}_2)\tilde{\mathbf{Z}}_\ell\hat{\mathbf{h}}_{\ell|\ell-1})$
16: Update covariance matrix,
$\hat{\mathbf{Q}}_\ell = (\mathbf{I}_2 - \tilde{\mathbf{K}}_\ell(\mathbf{P}^{\frac{1}{2}}_\ell \otimes \mathbf{I}_2)\tilde{\mathbf{Z}}_\ell\tilde{\mathbf{D}}_{\ell|\ell-1})\hat{\mathbf{Q}}_{\ell|\ell-1}$

[2]In our network deployment scenarios, the full set of RSUs, i.e., $\mathcal{U} = \{1,2,3\}$, wouldn't be used in the proposed joint tracking algorithm.

This article has been accepted for publication in IEEE Transactions on Vehicular Technology. This is the author's version which has not been fully edited and content may change prior to final publication. Citation information: DOI 10.1109/TVT.2022.3153345

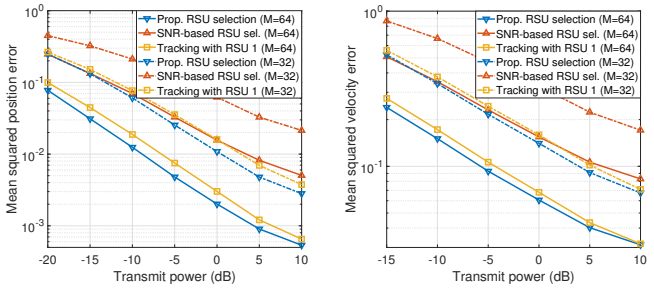

(a) Position tracking performance. (b) Velocity tracking performance.

Fig. 3. Mean squared errors of RSU selection systems in *Crossover Region B*.

on the predefined service areas in Fig. 2(c). The service areas for the SNR-based joint tracking system are predefined by substituting the SNR metric for the SANR metric in Algorithm 1, as depicted in Fig. 2(d). The service areas for both systems are designed to have the same surface area for joint tracking.

For a given set of selected RSUs $\mathcal{U} = \{u_1, \cdots, u_{|\mathcal{U}|}\}$, an input-output expression for the overall channel sounding process can be defined by

$$\tilde{\mathbf{r}}_\ell = [(\tilde{\mathbf{r}}_\ell^{u_1})^T, \cdots, (\tilde{\mathbf{r}}_\ell^{u_{|\mathcal{U}|}})^T]^T = (\mathbf{P}_\ell^{\frac{1}{2}} \otimes \mathbf{I}_2)\tilde{\mathbf{Z}}_\ell \tilde{\mathbf{h}}_\ell + \tilde{\mathbf{n}}_\ell \in \mathbb{R}^{2|\mathcal{U}|},$$

where $\mathbf{P}_\ell = \text{diag}([\rho_\ell^{u_1}, \cdots, \rho_\ell^{u_{|\mathcal{U}|}}])$ is a diagonal matrix for the set of average SNRs, $\tilde{\mathbf{Z}}_\ell = \tilde{\mathbf{Z}}_\ell^{u_1} \oplus \cdots \oplus \tilde{\mathbf{Z}}_\ell^{u_{|\mathcal{U}|}}$ is a block diagonal matrix for the overall combiner, $\tilde{\mathbf{h}}_\ell = [(\tilde{\mathbf{h}}_\ell^1)^T, \cdots, (\tilde{\mathbf{h}}_\ell^{u_{|\mathcal{U}|}})^T]^T$ is the overall channel vector, and $\tilde{\mathbf{n}}_\ell = [(\tilde{\mathbf{n}}_\ell^{u_1})^T, \cdots, (\tilde{\mathbf{n}}_\ell^{u_{|\mathcal{U}|}})^T]^T \sim \mathcal{N}\big(\mathbf{0}_{2|\mathcal{U}|}, \frac{\mathbf{I}_{2|\mathcal{U}|}}{2}\big)$ is the overall noise vector. The state update process is designed as

$$\hat{\mathbf{t}}_\ell = \hat{\mathbf{t}}_{\ell|\ell-1} + \tilde{\mathbf{K}}_\ell\big(\tilde{\mathbf{r}}_\ell - (\mathbf{P}_\ell^{\frac{1}{2}} \otimes \mathbf{I}_2)\tilde{\mathbf{Z}}_\ell \hat{\mathbf{h}}_{\ell|\ell-1}\big), \tag{9}$$

where $\hat{\mathbf{h}}_{\ell|\ell-1} = [(\tilde{\mathbf{h}}(\hat{\psi}_{\ell|\ell-1}^{u_1}))^T, \cdots, (\tilde{\mathbf{h}}(\hat{\psi}_{\ell|\ell-1}^{u_{|\mathcal{U}|}}))^T]^T$ is the overall predicted channel vector. The Kalman gain matrix is defined as

$$\tilde{\mathbf{K}}_\ell = \hat{\mathbf{Q}}_{\ell|\ell-1}\big((\mathbf{P}_\ell^{\frac{1}{2}} \otimes \mathbf{I}_2)\tilde{\mathbf{Z}}_\ell \tilde{\mathbf{D}}_{\ell|\ell-1}\big)^T \big((\mathbf{P}_\ell^{\frac{1}{2}} \otimes \mathbf{I}_2)\tilde{\mathbf{Z}}_\ell \tilde{\mathbf{D}}_{\ell|\ell-1} \hat{\mathbf{Q}}_{\ell|\ell-1}\big((\mathbf{P}_\ell^{\frac{1}{2}} \otimes \mathbf{I}_2)\tilde{\mathbf{Z}}_\ell \tilde{\mathbf{D}}_{\ell|\ell-1}\big)^T + \mathbf{I}_{2|\mathcal{U}|}/2\big)^{-1}. \tag{10}$$

Lastly, the covariance matrix is refined as

$$\hat{\mathbf{Q}}_\ell = (\mathbf{I}_2 - \tilde{\mathbf{K}}_\ell(\mathbf{P}_\ell^{\frac{1}{2}} \otimes \mathbf{I}_2)\tilde{\mathbf{Z}}_\ell \tilde{\mathbf{D}}_{\ell|\ell-1})\hat{\mathbf{Q}}_{\ell|\ell-1}.$$

A set of selected RSUs for joint tracking can be predefined because the overall SANR is a function of the vehicle position variables, $(\hat{x}_{\ell|\ell-1}, y)$, and the network design parameters, (X, Y, h). With the predicted state vector and the covariance matrix, $(\hat{\mathbf{t}}_{\ell|\ell-1}, \hat{\mathbf{Q}}_{\ell|\ell-1})$, each RSU can construct all the variables in (9) required for a joint tracking process, except the overall sample vector, $\tilde{\mathbf{r}}_\ell$. Based on the predefined service area for joint tracking, as depicted in Fig. 2(c), it is required to exchange sounding samples between RSUs to construct the overall sample vector in the joint state update process.

V. Simulation Results

The simulation results are presented to evaluate the performance of the proposed vehicle tracking algorithms. This study generates $10,000$ independent vehicle tracking scenarios. The

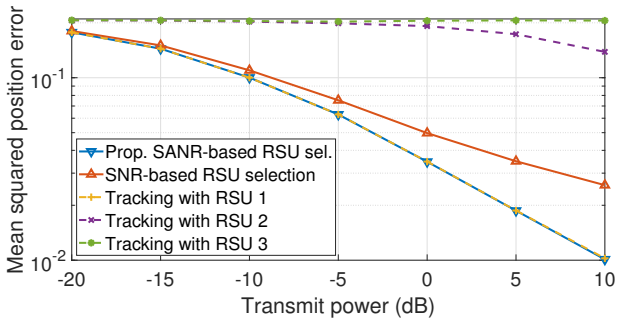

(a) Position tracking in *SANR-based RSU 1 Selection Area* with $(x_0, y) = (-75, 3.25)$ m.

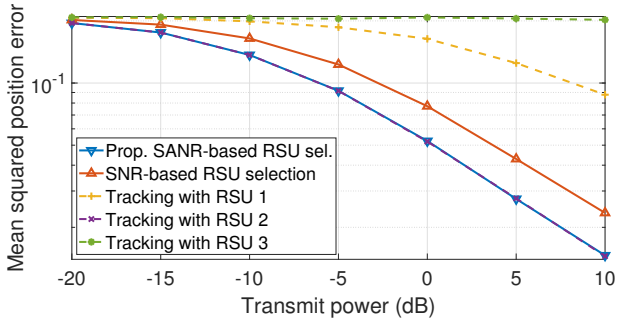

(b) Position tracking in *SANR-based RSU 2 Selection Area* with $(x_0, y) = (-80, 24.25)$ m.

Fig. 4. Mean squared position errors of vehicle tracking systems with $M = 32$ in *SANR-based RSU 1 or 2 Selection Areas*.

number of antennas at RSU is set to $M \in \{32, 64\}$. The radio signals at a center frequency $f_c = 28$ GHz employing 20 MHz bandwidth are utilized. The noise power is then calculated as, $\sigma_{\text{n}}^2 = -174 + 10\log_{10}(20 \times 10^6) \simeq -101$ dBm. The path-loss exponent is $n = 2$ and the sampling period for the uplink channel soundings is $T_s = 10$ ms. The channel vector consists of a line-of-sight and a non-line-of-sight radio path with Rician K factor, $K = 13$ dB. Similar to [10], the error parameters in (2) are set to $\{\sigma_\omega, \sigma_\alpha\} = \{10^{-1.5}, 0.05\big(v_0 \frac{10^3}{60^2}\big)\}$.

Before evaluating the joint vehicle tracking system, we present the tracking performances of the proposed SANR-based RSU selection algorithms within *Crossover Region B* in Fig. 2. The network design parameters are set to $(\text{X}, \text{Y}, h) = (75, 31, 7.5)$ m and an initial velocity of vehicle is set to $v_0 = 60$ km/h (16.67 m/s). In Figs. 3(a) and 3(b), the position and velocity tracking performances are evaluated, within a 2.5 s duration, by using the mean squared errors, $\Upsilon_x = \text{E}[|x_\ell - \hat{x}_\ell|^2]$ and $\Upsilon_v = \text{E}[|v_\ell - \hat{v}_\ell|^2]$, respectively. Fig. 3 shows that the proposed RSU selection algorithm using SANR gives better position and velocity tracking performances because both an average SNR and angular variation owing to vehicle movements are jointly considered to evaluate the vehicle tracking performance. The position estimation performance is better than the velocity estimation performance because the vehicle tracking algorithm is designed to use sounding samples written in terms of the position variables.

We evaluate position tracking performances by considering a single *Service Area* within a 1.5 s duration. We consider two different vehicle deployment scenarios, $(x_0, y) \in \{(-75, 3.25)\text{ m}, (-80, 24.25)\text{ m}\}$, in which RSUs are deployed

This article has been accepted for publication in IEEE Transactions on Vehicular Technology. This is the author's version which has not been fully edited and content may change prior to final publication. Citation information: DOI 10.1109/TVT.2022.3153345

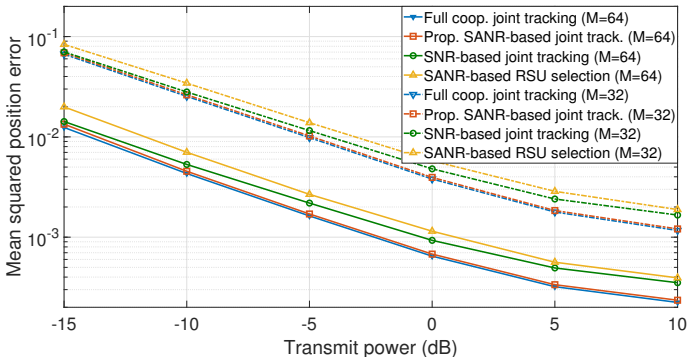

(a) Position tracking performance.

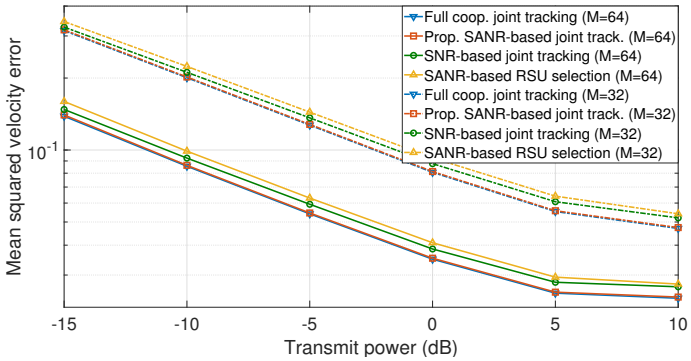

(b) Velocity tracking performance.

Fig. 5. Mean squared errors of vehicle tracking systems in *SANR-based RSU 1 & 2 Selection Areas*.

with the network design parameters, $(\mathrm{X}, \mathrm{Y}, h) = (125, 31, 7.5)$ m. In the proposed SANR-based RSU selection algorithm, the RSU 1 will always be chosen based on the SANR metric within *SANR-based RSU 1 Selection Area*. In Fig. 4(a), it is shown that there are no performance gap between the proposed RSU selection algorithm and the vehicle tracking system exploiting only RSU 1. For the above mentioned reasons, in Fig. 4(b), the proposed RSU selection system and the vehicle tracking system exploiting only RSU 2 produce the same vehicle tracking performances because the RSU 2 will always be chosen based on the SANR metric within *SANR-based RSU 2 Selection Area*.

Lastly, a vehicle tracking performance of the proposed joint tracking system is evaluated in *SANR-based RSU 1 & 2 Selection Areas*. The network design parameters are set to $(\mathrm{X}, \mathrm{Y}, h) = (75, 31, 7.5)$ m and an initial state vector is given by $\mathbf{t}_0 = [-60 \text{ m}, \ 60 \text{ km/h}]^T$ with $y = 3.25$ m. A vehicle departs from the point within *SANR-based RSU 2 Selection Area* and arrives in *SANR-based RSU 1 Selection Area* after driving for 2.5 seconds. As shown in Fig. 5, the joint tracking systems provide better performance than previous tracking systems exploiting a single RSU because the changes in multiple beam directions are considered jointly for tracking vehicle movements. The mean squared error decreases with increasing beamforming gain by exploiting more antennas at RSUs. The proposed SANR-based joint tracking system with $\tau_{\text{th}} = 0.98$ and the SNR-based joint tracking system with $\tau_{\text{th}} = 0.662$ exploit 1.5 sounding samples for joint vehicle tracking. On the other hand, in the full cooperative tracking system, a vehicle tracking is performed by using sounding samples received from three RSUs. It is verified that the performance gap between the proposed joint tracking system and the full cooperative tracking system is negligible, although the proposed system exploits far less sounding samples. Furthermore, the proposed SANR-based joint tracking system outperforms the SNR-based joint tracking system that exploits similar amounts of samples. Numerical results verify that the proposed SANR-based system enhances the vehicle tracking performance while minimizing the amount of sounding sample exchange.

VI. Conclusion

We developed the joint vehicle tracking and RSU selection algorithms by considering a massive RSU deployment scenario in V2I networks. The vehicle tracking performance was analyzed as a function of the angular derivative of the dominant radio path in a spatial frequency domain and the SNR. Based on the derived metric, we developed an RSU selection algorithm that can maximize the vehicle tracking performance by considering the relative position between a vehicle and RSUs. Moreover, a joint vehicle tracking algorithm was developed to track vehicle movements more reliably while minimizing the exchange of sounding samples between RSUs. The proposed joint tracking and RSU selection algorithms outperformed conventional SNR-based vehicle tracking systems.

References

[1] J. Zhang, F. Wang, K. Wang, W. Lin, X. Xu, and C. Chen, "Data-driven intelligent transportation systems: A survey," *IEEE Trans. on Intelligent Transportation Systems*, vol. 12, no. 4, pp. 1624–1639, Dec. 2011.

[2] TS-22.186, *Enhancement of 3GPP support for V2X scenarios*, Std., 2019.

[3] J. Choi, V. Va, N. Gonzalez-Prelcic, R. Daniels, C. R. Bhat, and R. W. Heath, "Millimeter-wave vehicular communication to support massive automotive sensing," *IEEE Communications Magazine*, vol. 54, no. 12, pp. 160–167, Mar. 2016.

[4] M. Kutila, P. Pyykonen, Q. Huang, W. Deng, W. Lei, and E. Pollakis, "C-V2X supported automated driving," in *Proceedings of IEEE International Conference on Communications Workshops (ICC Workshops)*, May 2019.

[5] J.-H. Lee and J. Song, "Full-duplex relay for millimeter wave vehicular platoon communications," *Sensors*, vol. 20, no. 21, pp. 1–15, Oct. 2020.

[6] T. Noguchi, Y. C. Ting, M. Yoshida, and A. G. Ramonet, "Real-time cooperative vehicle tracking in VANETS," in *Proceedings of International Conference on Computer Communications and Networks (ICCCN)*, Aug. 2020.

[7] T. Zeng, O. Semiari, W. Saad, and M. Bennis, "Joint communication and control system design for connected and autonomous vehicle navigation," in *Proceedings of IEEE International Conference on Communications (ICC)*, May 2019.

[8] V. Va, H. Vikalo, and R. W. Heath, "Beam tracking for mobile millimeter wave communication systems," in *IEEE Global Conference on Signal and Information Processing (GlobalSIP)*, Dec. 2016.

[9] S. Shaham, M. Ding, M. Kokshoorn, Z. Lin, S. Dang, and R. Abbas, "Fast channel estimation and beam tracking for millimeter wave vehicular communications," *IEEE Access*, vol. 7, Sep. 2019.

[10] S.-H. Hyun, J. Song, K. Kim, J.-H. Lee, and S.-C. Kim, "Adaptive beam design for V2I communication using beam tracking with extended Kalman filter," vol. 71, no. 1, pp. 489–502, Jan. 2022.

[11] J. Barrachina, P. Garrido, M. Fogue, F. J. Martinez, J. C. Cano, C. T. Calafate, and P. Manzoni, "Road side unit deployment: A density-based approach," *IEEE Intelligent Trans. Systems Magazine*, vol. 5, no. 3, 2013.

[12] J. H. Choi, Y. H. Han, and S. G. Min, "A network-based seamless handover scheme for vanets," *IEEE Access*, vol. 6, Sep. 2018.

[13] R. Irmer, H. Droste, H. Marsch, M. Grieger, G. Fettweis, S. Brueck, H. P. Mayer, L. Thiele, and V. Jungnickel, "Coordinated multipoint: Concepts, performance, and field trial results." *IEEE Communications Magazine*, vol. 49, no. 2, pp. 102–111, Jul. 2011.

[14] K. Saho, *Kalman filter for moving object tracking: Performance analysis and filter design*. InTech, 2018.